Photophysics of novel diamond based single photon emitters

I. Aharonovich, S. Castelletto, D. A. Simpson, A. D. Greentree and S. Prawer

School of Physics, The University of Melbourne, 3010 Victoria, Australia

i.aharonovich@pgrad.unimelb.edu.au, sacas@unimelb.edu.au

Abstract: A detailed study of the photophysical properties of several novel color centers in chemical vapor deposition diamond is presented. These emitters show narrow luminescence lines in the near infra-red. Single photon emission was verified with continuous and pulsed excitation with emission rates at saturation in the MHz regime, whilst direct lifetime measurements reveal excited state lifetimes ranging from 1-14 ns. In addition, a number of quantum emitters demonstrate two level behavior with no bunching present in the second order correlation function. An improved method of evaluating the quantum efficiency through the direct measurement of the collection efficiency from two level emitters is presented and discussed.

OCIS codes: (270.0270) Quantum optics; (270.5290) Photon Statistics; (160.4760) Optical properties; (170.1790) Confocal microscopy

References and links

1. S. Strauf, N. G. Stoltz, M. T. Rakher, L. A. Coldren, P. M. Petroff and D. Bouwmeester, "High-frequency single-photon source with polarization control", Nat. Photonics **1**, 704 (2007).
2. C. Santori, M.Pelton, G. Solomon, Y. Dale and Y. Yamamoto, "Triggered single photons from a quantum dot", Phys. Rev. Lett. **86**, 1502(2001)
3. C. Brunel, B. Lounis, P. Tamarat, M. Orrit,"Triggered source of single photons based on controlled single molecule fluorescence", Phys. Rev. Lett. **83**, 2722 (1999)
4. A. Tribu, G. Sallen , T. Aichele, R. Andre, J. P.Poizat, C. Bougerol, S. Tatarenko and K. Kheng, "A High-Temperature Single-Photon Source from Nanowire Quantum Dots", Nano Lett. **8**, 4326 (2008).
5. C. Kurtsiefer, S. Mayer, P. Zarda and H. Weinfurter,"Stable Solid State source of Single Photons" **85**, 290 (2000).
6. A. Beveratos, S. Kuhn, R. Brouri, T. Gacoin , J. P. Poizat and P. Grangier, "Room temperature stable single-photon source", Eur. Phys. J. D **18**, 191 (2002).
7. A. M. Zaitsev, "Optical Properties of Diamond," A Data Handbook, Springer, Berlin, 2001
8. F. Jelezko, J. Wrachtrup,"Single defect centres in diamond: A review",Phys. Stat. Sol. **203**, 3207 (2006).
9. C. L. Wang, C.Kurtsiefer, H. Weinfurter and B. Burchard, "Single photon emission from SiV centres in diamond produced by ion implantation", J. Phys.B **39**, 37 (2006).
10. T. Gaebel,I. Popa, A. Gruber, M. Domhan, F. Jelezko and J. Wrachtrup, "Stable single-photon source in the near infrared" New J. Phys. **6**, 98 (2004).
11. E. Wu, V. Jacques, H. Zeng, P. Grangier, F. Treussard and J.F. Roch,"Narrow-band single-photon emission in the near infrared for quantum key distribution", Opt. Expr. **14**, 1296 (2006).
12. E. Wu, J.R. Rabeau, G.Roger, F.Treussart, H. Zeng, P.Grangier, S. Prawer and J. F. Roch, "Room temperature triggered single-photon source in the near infrared", New J. Phys. **9**, 434 (2007).
13. I. Aharonovich, C. Zhou, A.Stacey, F. Treussart, J. F. Roch and S. Prawer, "Formation of color centers in nanodiamonds by plasma assisted diffusion of impurities from the growth substrate" Appl. Phys. Lett. **93**, 243112 (2008).

14. D. A. Simpson, E. Ampem-Lassen, B. C. Gibson, S. Trpkovski, F.M. Hossain, S. T. Huntington, A. D. Greentree, L. C. L. Hollenberg and S. Prawer, "A highly efficient two level diamond based single photon source", Appl. Phys. Lett **94**, 203107 (2009).
15. I. Aharonovich, S. Castelletto, D. A. Simpson, A. Stacey, J. McCallum, A. D. Greentree and S. Prawer, "Two-level ultra bright single photon emission from diamond nanocrystals," Nano Lett. in press.
16. J. Y. Cheung , C. J. Chunnilall ,E. R. Woolliams , N. P. Fox , J. R. Mountford , J. Wang a, P. J. Thomas,"The quantum candela: a re-definition of the standard units for optical radiation", J. of Mod. Opt. **54**, 373-396 (2007)
17. S.Schietinger, M.Barth, T. Aichele and O. Benson, "Plasmon-Enhanced Single Photon Emission from a Nanoassembled Metal-Diamond Hybrid Structure at Room Temperature", Nano Lett. **9**, 1694 (2009).
18. S.Schietinger, T. Aichele and O. Benson, "One-by-One Coupling of Single Defect Centers in Nanodiamonds to High-Q Modes of an Optical Microresonator", Nano Lett. **1**, 3911 (2008).
19. S. C. Kitson, P. Jonsson, J. G. Rarity, and P. R. Tapster,"Intensity fluctuation spectroscopy of small numbers of dye molecules in a microcavity", Phys. Rev. A **58**, 620 (1998)
20. A. Beveratos, S. Kuhn, R. Brouri, T. Gacoin , J. P. Poizat and P. Grangier, "Nonclassical radiation from diamond nanocrystals", Phys. Rev. A Rapid Comm. **64** , 061802R (2001).
21. A. Stacey, I. Aharonovich, S. Prawer, J. E. Butler, "Controlled synthesis of high quality micro/nano-diamonds by microwave plasma chemical vapor deposition", Diam. and Rel. Mat. **18**, 51 (2009).
22. A. M. Zaitsev, "Vibronic spectra of impurity-related optical centers in diamond", Phys. Rev. B, **61**, 12909 (2000).
23. C. Santori, D. Fattal, S. M. Spillane, M. Fiorentino, R.G. Beausoleil, A.D. Greentree, P. Olivero, M. Draganski, J.R. Rabeau, P. Reichart, B.C. Gibson, S. Rubanov, D.N. Jamieson, S. Prawer, "Coherent population trapping in diamond N-V centers at zero magnetic field", Opt. Exp. **14**, 7986 (2006)

1. Introduction

The emerging field of quantum optics has established a demand for an accessible solid state system which can generate a stream of single photons on demand [1]. Although single photon emission has been demonstrated from quantum dots (QD) [1, 2],single molecules [3] and nanowires[4], the operation of those systems is often limited by the temperature. Diamond crystals, on the other hand, offer the most promising platform for generation of robust, photo stable, single photons at room temperature [5, 6]. Nevertheless, out of more than 500 existing optical centers in diamond [7], only three known centers demonstrate single photon emission, namely, the nitrogen-vacancy complex [8, 6], the silicon-vacancy complex [9] and the nickel-nitrogen complex [10, 11, 12].

Recent progress in materials science and fabrication techniques of diamond color centers [13] unveiled novel quantum emitters operating in the MHz regime [14, 15]. These new centers, are comparable to QD in terms of brightness [1], but have the tremendous advantage of stable operation at room temperature. These break throughts have opened a new avenue to investigate essentially an unknown group of single photon emitters in diamond.

The simple two-level nature of a select few single photon emitters allows a direct estimate of the collection efficiency associated with the optical setup, the precise knowledge of the collection efficiency can lead to more accurate estimations of the quantum efficiency of the more common three level single photon emitting systems. This type of source can thus eventually be used as a reference for an absolute characterization of the quantum efficiency along with more precise estimations of the collection efficiency of the system, provided the photo-physics is well understood. One can envisage that single photon sources could be implemented as a "single photon standard", able to link classical radiometric measurements to the fundamental quantum optical entities. In particular in the long term such a single photon standard could contribute to a re-definition of the standard units for optical radiation in terms of the "quantum candela" [16]. The controlled fabrication of the MHz class of diamond single photon emitters, together with a recent emission enhancement by coupling the light to plasmonic structures [17] or cavities [18], is expected to progress the technology beyond the point in which they can become practical quantum information and metrology devices.

In this paper, a detailed study of the photophysical properties of the novel family of single photon emitters reported in [15] has been undertaken. To gain insight into the electronic

level structure of the emitters, their fundamental optical properties such as lifetime, photoluminescence (PL) spectrum, sub-poissionian statistics and saturation count rate have been studied and compared. We concentrate on the typical PL lines in the range of 740-770 nm, which exhibit single photon emission with count rates ranging from 1.3-3.2 10^6 counts/s at saturation.

2. Theoretical background

The physics of the photoluminescence emitted from a single diamond color center can be described within the framework of a two level system comprising a ground and excited state, and in many instances as a three-level system [5, 11, 19], whereby the single center is excited from its ground state to the excited state, with a third longer lived state providing an additional decay path from the excited state, as seen in Fig. 1. The rate equations describing the populations of

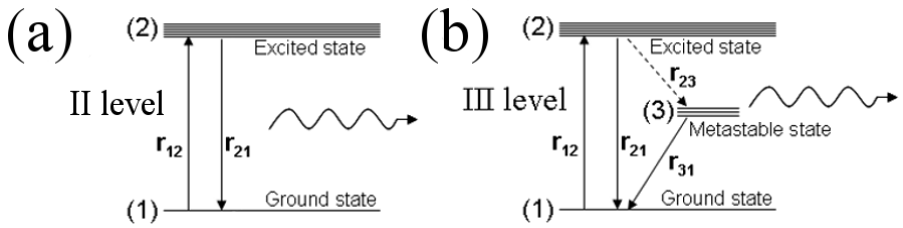

Fig. 1. Schematic diagram of a (a) two-level and (b) three-level system, where r_{nm} $n,m = 1,2,3$ are the transition rates from level (n) to level (m).

the two and three level systems can be written in matrix form as:

$$\begin{pmatrix} \dot{n_1} \\ \dot{n_2} \end{pmatrix} = \begin{pmatrix} -r_{12} & r_{12} \\ r_{12} & -r_{21} \end{pmatrix} \begin{pmatrix} n_1 \\ n_2 \end{pmatrix} \tag{1}$$

and

$$\begin{pmatrix} \dot{n_1} \\ \dot{n_2} \\ \dot{n_3} \end{pmatrix} = \begin{pmatrix} -r_{12} & r_{21} & r_{31} \\ r_{12} & -r_{21}-r_{23} & 0 \\ 0 & r_{23} & -r_{31} \end{pmatrix} \begin{pmatrix} n_1 \\ n_2 \\ n_3 \end{pmatrix}. \tag{2}$$

By solving Eqs (1) and (2) with the initial condition $n_1 = 1, n_2 = 0, n_3 = 0$ (i.e the system is prepared in the ground state), the instantaneous emission probability of a photon being emitted from the excited state, $n_2(t)$, can be obtained. By normalizing $n_2(t)$ to the probability of a photon being emitted at an infinite time $n_2(\infty)$ an analytical expression describing the second order correlation function can be obtained. The respective analytical expressions for the two and three level [11, 19] cases are then given by:

$$g^{(2)}(\tau) = 1 - \exp(-\lambda_1 \tau). \tag{3}$$

where $\lambda_1 = r_{12} + r_{21}$ and

$$g^{(2)}(\tau) = 1 - (1+a)\,\exp(-\lambda_1 \tau) + a\,\exp(-\lambda_2 \tau), \tag{4}$$

where $\lambda_2 = r_{31} + r_{23} r_{12}/\lambda_1$, and $a = r_{12} r_{23}/(\lambda_1 r_{31})$.

The decay rate λ_1 depends on the excitation optical power, P_{opt} as:

$$\lambda_1 = r_{21}^0 (1 + \alpha P_{\text{opt}}), \tag{5}$$

where r_{21}^0 is the inverse of the excited state lifetime (τ_{21}) and α is a fitting parameter.

Similarly, for the three-level system, the decay rate λ_2, assuming r_{23} constant with the excitation power [11], can be written in terms of r_{31}^0 in the limit of zero optical power.

$$\lambda_2 = r_{31}^0(1+\beta P_{\text{opt}}) + \frac{r_{23}r_{12}}{r_{21}^0(1+\alpha P_{\text{opt}})}, \tag{6}$$

where β is a fitting parameter.

With an accurate determination of the second order correlation function one can determine the individual decay rates involved in the system and gain an understanding of the energy level structure. Upon inspection of the two and three level auto-correlation functions there is a clear distinction in the shape and nature of the exponential component. In the two level case the function exhibits a simple exponential rise at a rate equivalent to the fluorescence decay rate of the excited state in the limit of zero optical excitation i.e. $r_{12} \to 0$, with the exponential asymptotic to a $g^{(2)}(\tau)$ value of 1. The three level expression, on the other hand, contains two exponential components each with a characteristic time constant. Depending on the transition rates from the excited state to the shelving state and shelving state back to the ground state, $g^{(2)}(\tau)$ can increase beyond 1 for times $> \tau_{21}$, before decaying back to 1 at times $>> \tau_{21}$.

The phenomenon of $g^{(2)}(\tau)$¿1 is commonly termed “photon bunching” and this behavior enables a clear distinction to be made between two and three level systems. The second order correlation function describes the probability of detecting a photon with a delay time τ after one photon has been detected at τ=0. Hence, the bunching effect describes the enhanced probability to detect a photon at short times then at longer times. Indeed after the system undergoes a transition to its shelving state, which has longer lifetime, there is a longer interval between the photons. Once the system relaxed to the ground state and undergo a full emission cycle again, the normal photon rate is achieved again. The waiting interval while the system in the metastable state thus creates the bunching effect of the $g^{(2)}(\tau)$.

The measurement $g^{(2)}(\tau)$ is done typically using a Hanbury-Brown and Twiss (HBT) interferometer whereby the coincidence events of two detectors are measured. In practice, the temporal jitter of the detectors and of the electronics can be ignored provided that the lifetime is much longer than the temporal jitter; with the identification of emitting centers with increasing short fluorescence lifetimes [9, 11, 13], the effect of the temporal jitter on the measured auto-correlation function $g^{(2)}_{\text{meas}}(\tau)$ must be taken into account. Therefore the measured auto-correlation function is given by the convolution of Eqs (3,4) with the instrumental time response function $J(\tau)$:

$$g^{(2)}_{\text{meas}}(\tau) = \int_{-\infty}^{\infty} \mathrm{d}\tau' g^{(2)}(\tau') J(\tau - \tau'). \tag{7}$$

The majority of single photon emitters identified in diamond (such as: Si-V [9], NV [20] and the NE8[10, 11]) have been attributed to three level systems which suffer from quenching due to the presence of a shelving state. However, the recent identification of highly efficient two level systems in diamond [13, 14] has attracted considerable interest, particularly due to its central role in determining more accurately the collection efficiency of the setup and the quantum efficiency of three level systems. The quantum efficiency, η_{QE}, of an emitter is defined as the probability of an absorbed pump photon resulting in emitted photon. For a two level emitter, the quantum efficiency is equal to 1 when $r_{12} >> r_{21}$, indicating that for each absorbed pump photon a photon is emitted from the excited state.

We can deduce the number of emitting photons or the fluorescence count rate of a two level

system by solving the rate equations in Eq. (1):

$$\phi = \frac{\phi_\infty P_{\text{opt}}}{P_{\text{sat}} + P_{\text{opt}}}, \tag{8}$$

where ϕ represents the single photon count rate, $\phi_\infty = r_{21}^0 \eta$, is the saturation count rate for $P_{\text{opt}} \rightarrow \infty$ where η represents the total collection efficiency and $P_{\text{sat}} = \alpha^{-1}$ is the optical saturation power.

In the three level case the quantum efficiency can be derived analytically in terms of the detected fluorescence rate by solving the rate equations in Eq. (2):

$$\phi = \eta_{QE} \times \eta \frac{r_{21}}{1 + \frac{r_{21}}{r_{12}} + \frac{r_{23}}{r_{31}}}. \tag{9}$$

3. Experiment

The CVD diamond crystals employed in this work were grown to an average size of few hundreds nanometers from diamond seeds (4-6 nm) on a sapphire substrate using a microwave plasma enhanced CVD technique (900 W, 150 Torr)[21]. A home built confocal microscope with a spatial resolution $\sim$ 400 nm and HBT interferometer were used to identify the emitting centers and measure the time correlation of photoluminescence (PL) intensity (Fig. 2(a)). A fiber coupled CW diode laser emitting at 682 nm and a 690 nm pulsed diode 200 ps pulse width (repetition rate from 10 MHz up to 80 MHz) were interchanged for excitation. The lasers polarization was controlled by a Glan Taylor polarizer and a half-wave plate. The diamond sample was mounted on a piezo XYZ stage with 0.2 nm resolution, allowing 100x100 μm^2 scans. The unwanted residual laser line was eliminated by a dichroic beam splitter and a F_1 broad (10 nm FWHM) band-pass filter centred at 740 nm, 749 nm or 760 nm depending on the PL from a specific crystal. The PL from the emitting centers was then coupled into a 62.5 μm core multimode fiber, which acts as an aperture. A 50:50 fibre coupled beam splitter guided the photons to two single photon counting detectors (APDs) and their outputs were sent to the start and stop inputs of the time correlator card. The PL was recorded without the bandpass F_1 filter using a fiber-coupled spectrometer with a cooled CCD array. All the measurements were performed at room temperature.

4. Results

More than 10 different sapphire substrates were scanned, with crystals grown to a size of a few hundred nanometers. Fig. 2b shows a typical confocal map of the diamond crystals obtained by 682 nm laser excitation. The PL spectra of the bright spots revealed emission with zero phonon lines (ZPLs) centered at 744$\pm$2 nm (FWHM $\sim$ 11nm),749$\pm$2 nm (FWHM $\sim$ 4nm), 756$\pm$2 nm (FWHM $\sim$ 11 nm), and 764$\pm$2 nm (FWHM $\sim$ 10 nm), as shown in Fig. 3. In some cases two or more of these lines were found in one crystal, as shown in the inset of Fig. 3. Anti-bunching measurements on crystals containing multiple emission lines generally showed multiple emitters with auto-correlation functions at the zero delay time of $g^{(2)}(0) > 0.5$, with the intensity of the lines varying from crystal to crystal. These characteristic emission lines are in agreement with cathodo-luminescence lines from chromium related centers in diamond, exhibiting narrow lines in the region of 740-770 nm [22].

Figure 4(a-d) show the antibunching behavior of the PL lines centered at 744 nm, 749 nm, 756 nm and 764 nm measured with the HBT interferometer for excitation powers below and above the optical saturation power P_{sat}. The dip at zero delay time indicates a single photon emitter. The raw coincidence data were corrected for the background as described in ref. [6].

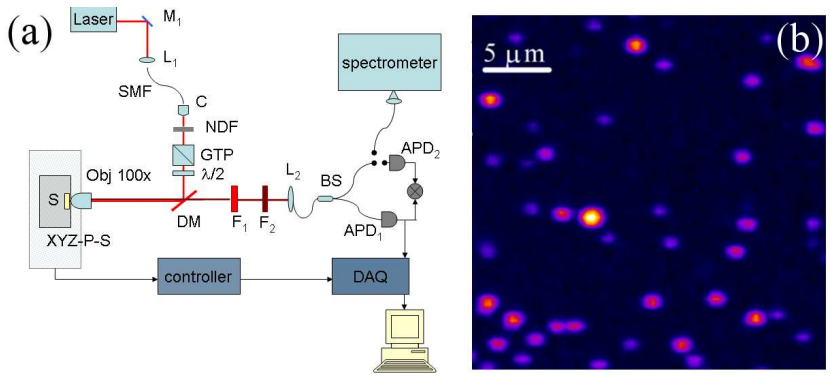

Fig. 2. (a)Experimental setup. A diode laser at 682 nm operating in CW and a pulsed 690 nm laser were alternatively coupled to a single mode fiber, and then collimated (C) and polarized by a Glan Taylor polarizer (GTP). The laser polarization was varied by an half-wave plate ($\lambda/2$). A variable neutral density filter (NDF) was used to change the excitation power. Samples (S) were excited by focusing the laser light by a high numerical aperture (0.9) objective with 100x magnification. A dichroic mirror (DM)transmitting from 720 nm, was used to separate the laser line form the sample fluorescence emission, when collected back from the same Obj. $F_{1,2}$ are band-pass filters, 794±80 nm and alternatively 760±12 nm or 740±12 nm, to isolate the single photon emission lines. A 100 mm focal length lens was used to send the single photon emission to a multimode-fiber, providing an aperture for the confocal imaging. Finally a 50:50 fiber beam splitter was used to verify the single photon emission by performing the auto-correlation between two low-dark counts (150 counts/s) single photon counting modules (APD). The S were mounted on a Physics Instruments XYZ piezo stage in closed loop operation. (b) Confocal image of 20x20 μm^2 showing bright spots which corresponds to a color center within a diamond crystal.

Due to the observed bunching, the center with a ZPL at 749 nm was fit by Eq.(4) and Eq.(7),which describes three level model. The other three centers, which exhibit two level behavior, were fit by Eq.(3) and Eq.(7). The deviation from zero of the auto-correlation function is attributed to the jitter of the electronics and detectors and residual polarisation dependent background.

The $g^{(2)}_{\mathrm{meas}}(0)$ of the 744, 749, 756 and 764 nm centers were 0.44, 0.16, 0.2, and 0.09, respectively. The excited state lifetime of the 744, 756 and 764 nm emitters were 3.8, 3.7 and 13 ns, respectively and were obtained by extrapolating the decay rate λ_1 to zero optical power, refer to Eq. 5, see Fig. 5. The fit applied to the second order correlation function for the 749 nm emitter contains two exponential decay rates λ_1 and λ_2. The extrapolation of these rates to zero optical excitation allows the excited state lifetime and shelving decay rates to be determined. The decay rate λ_2 as a function of optical power is shown in the inset of Fig. 5. The resulting values of r^0_{31} and r_{23} are 6.2 MHz and 0.89 MHz, respectively and are much smaller than the excited state decay rate, obtained from λ_1, r^0_{21}=880 MHz (τ_{21} = 1.1 ns).

The single photon emission count rate as a function of optical power P_{opt} is shown for each emitter in Fig.6. The measured count rates (corrected for the background) are given by the sum of the counts on the two APDs in the HBT setup. For the 744, 756 and 764 nm emitters, the saturation curves were fit according to Eq.(8) yielding saturation count rates ϕ_∞ of 2.1×10^6, 3.2×10^6 and 1.3×10^6 counts/s, respectively. The saturation curve of the three level 749 nm emitter was fit using Eq.(9), with the values of $r_{21}, r_{12}, r_{31}, r_{23}$ obtained from the fit to $g^{(2)}_{\mathrm{meas}}(\tau)$ as a function of pump power and the value η obtained as discussed in the following text. The

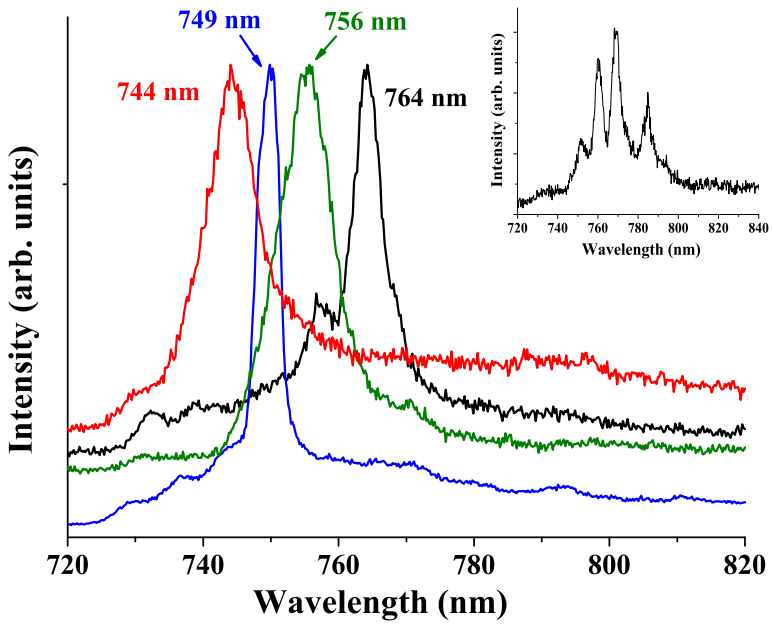

Fig. 3. Typical PL spectra recorded from individual CVD diamond crystals as shown in the raster scan of the sample in Fig. 1. The peak emission lines centred at 744 nm (red), 749 nm (blue), 756 nm (green) and 764 mn (black). Similar emission lines were also found all together in one crystal (inset).

single fitting parameter η_{QE} was then obtained from a least squares fit to the saturation curve.

Figure 7 shows a direct measurement of the lifetime recorded from the emitters using the pulsed excitation at 20 MHz repetition rate. The single exponential fit to the fluorescence decay of each emitter, resulted in measured excited state lifetimes of 4.1 ns, 1.4 ns and 14.2 ns for the 744 nm, 749 nm and 764 nm centres, respectively. Upon inspection of the fluorescence decay of the 744 and 749 nm centres there is a fast component of the fluorescence decay which occurs on a time scale less than 0.5 ns, this component is attributed to the background within the emitting crystal. The lifetime of the emitter is this case is determined by fitting the fluorescence decay for times greater than 0.5 ns. The long fluorescence lifetime of the 764 nm centre mitigates this effect and the decay can be described well by the single exponential fit. The measured lifetimes are in a good agreement with the lifetimes estimated from the CW measurements for the 744 nm and 749 nm emitters. The discrepancy with the 764 nm centre can be due to the lack of the CW $g^{(2)}(\tau)$ measurements at excitation powers well below saturation, which affects the fit to a zero excitation power.

In the inset of Fig. 7 is an example of the second order correlation function measurement under pulsed excitation from the 749 nm emitting crystal. The peak at τ=0 is the probability of having two photons in the same pulse, indicating in this case the presence of only one photon($g^{(2)}(0) = 0.17$). The observed deviation from zero is due the background luminescence from the diamond crystals, which is not negligible in this case. A pulsed measurement is mandatory for quantum optics application since single photons on demand (triggered single photons) are required. To reduce the unwanted background for practical application, temporal filtering of our single photon source can be implemented.

The total collection efficiency, η, of our setup can been measured directly by exciting a

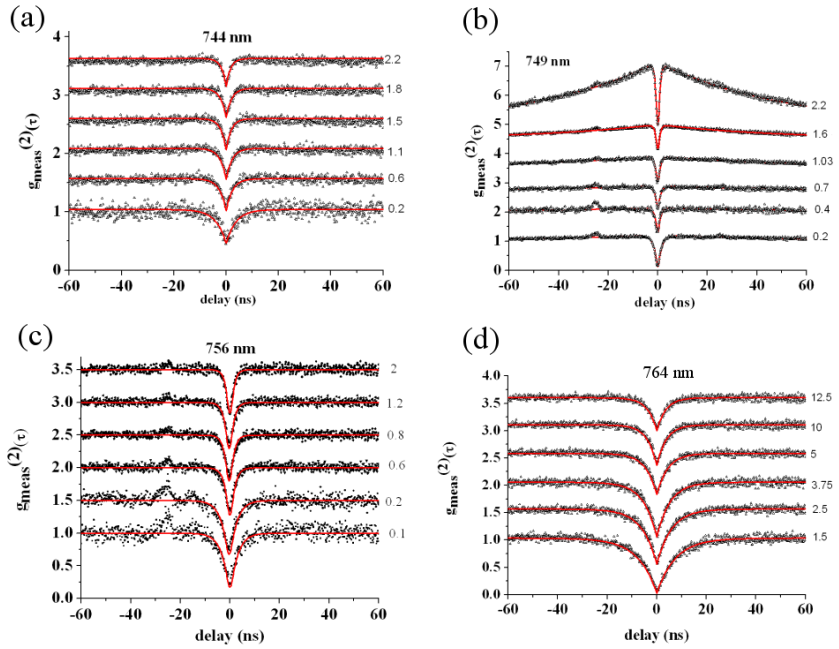

Fig. 4. Background corrected second-order auto-correlation function $g^{(2)}_{\text{meas}}(\tau)$, measured with 154 ps coincidence time bin for 300 s at different optical powers for the (a) 744 nm line, (b) 749 nm line the (c) 756 nm line and the (d) 764 nm line. The data of the 749 nm line was fit by Eq.(4,7), while the data of the 744 nm, 756 nm and 764 nm lines were fit by Eq.(3,7). The number to the right of the curves correspond to $P_{\mathtt{opt}}/P_{\mathtt{sat}}$

two level emitter in the pulsed regime. The total collection efficiency can be described by $\eta = \eta_{\text{opt}} \times \eta_{\text{det}} \times \eta_\theta \times \eta_{\text{cr}}$, where η_{opt} corresponds to the optical transmittance, η_{det} is the detection efficiency, η_θ corresponds to the geometrical efficiency, associated to the matching between the collection optics numerical aperture and the source spatial distribution and η_{cr} accounts for the crystal geometry, that contributes to the orientation of the excitation dipole of the center with respect to the excitation electric field and the emission dipole with respect to the collection optics. These are the limiting parameters that reduce the collection efficiency of the source down to typically a few percent.

In the case of a two-level system the total collection efficiency can be measured directly, as each excitation pulse generates one emitted photon (without being trapped in the metastable state), hence the absence of detected photons is a directly related to η. In the condition where the laser excitation energy is above saturation, the laser pulses temporal separation is longer than the typical detectors dead time (50 ns) and the source lifetime (14.2 ns), the total collection efficiency can be directly measured from the total count rate and the laser repetition rate $\eta = \phi/R_{rep}$. As an example, exciting the 764 nm with a laser repetition rate of 10 MHz, η =1.5% is obtained. Similarly, in the CW regime, η is given by $\eta = \phi_\infty/(r^0_{21})$. By calculating η for each two level emitter, an average value of η=1.3% is obtained. The discrepancy in the value of collection efficiency for various two level emitters may be attributed to a variation in η_{cr} due to the unknown dipole orientation of the emitter within the crystal and/or residual polarisation dependent background, that can influence the total saturation count rate ϕ_∞. The accuracy of η_{cr} can be improved by engineering centers with a known dipole orientation and

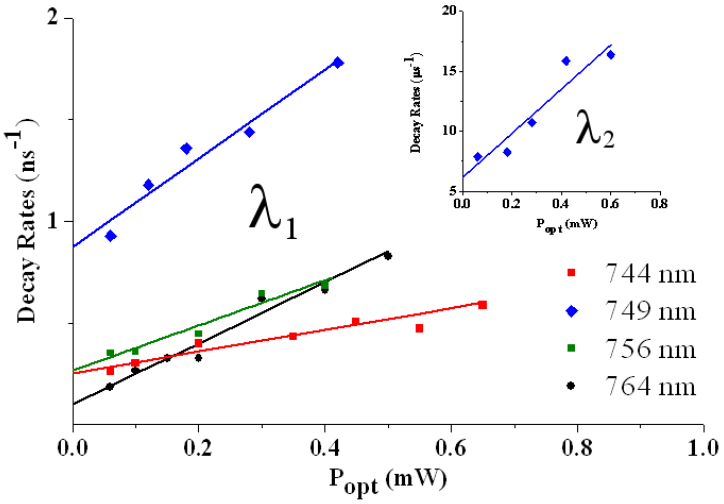

Fig. 5. Estimated λ_1 parameters for the centers at 744 nm (red squares), 749 nm (blue diamonds), 756 nm(green triangles) and 764 nm (black circles) versus the optical power. At the limit of zero optical power the lifetimes of the centers are respectively $(r_{21}^0)^{-1}$=3.8 ns, 1.1 ns, 3.7 ns, and 13 ns. The data were fit with Eq.(5). The behavior of λ_2 versus the optical power of the emitters at 749 nm is also shown inset and fit with Eq.(6); the estimated values r_{31}^0 =6.2 MHz (161 ns), and r_{23}=0.89 MHz (1.1 μs), $\alpha = 2.5$ mW^{-1}, $\beta = 3.1$ mW^{-1}.

lower fluorescent background. A detailed analysis of the various parameters of the collection efficiency, which is beyond the scope of the paper, is however important to exploit fully the two-level system properties for improving measurement accuracy. After identifying the collection efficiency η=1.3%, the quantum efficiency η_{QE}=0.24 of the 749 nm emitter is derived from the fit to the saturation curve with Eq.(9).

A summary of the photo-physics parameters for each single emitter is shown in Table 1. The ratio between the average off and on periods of the source is given by the ratio r_{23}/r_{31}

Table 1. Summary of the photo-physics parameters

λ (nm)	η_{QE}	ϕ_∞ (counts/s)	τ_{21} (ns) (pulsed)	τ_{21} (ns) (CW)	r_{31} (MHz)	r_{23} (MHz)
744	1	2.1 10^6	4.1	3.8		
756	1	3.2 10^6		3.7		
764	1	1.3 10^6	14.2	13		
749	0.24	2.7 10^6	1.4	1.1	6.2	0.89

which equals to 0.14 for 749 nm emitter. This value indicates that the probability of transition to the metastable state is moderate, as shown by the slight bunching of the $g^{(2)}(\tau)$ function (Fig. 4b). Previous determinations associated to NE8 complex in bulk natural diamond IIa [10, 11], and CVD nanodiamond [12] showed r_{23}/r_{31} of 2.8, 1.6 and 0.8 respectively, justifying much lower saturation rates of NE8 with respect to the 749 nm center. In addition, the center possess a shorter lifetime than NE8, which also contributes to the higher emission rates despite the

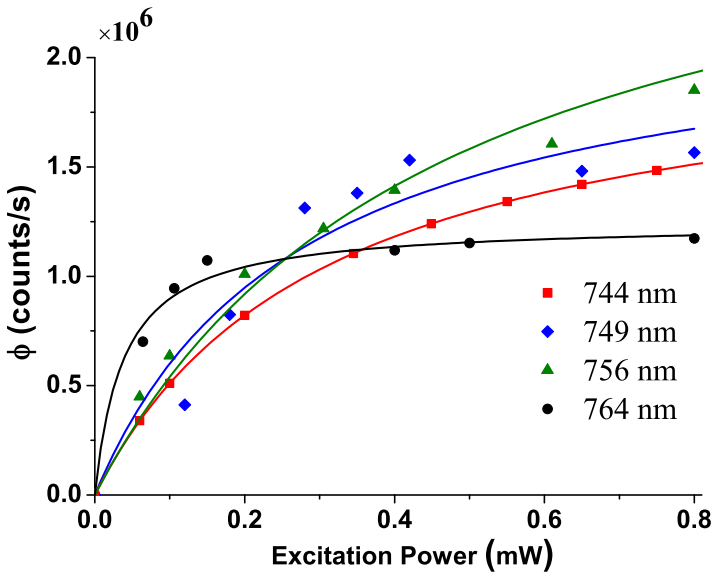

Fig. 6. Measured saturation curves and fit according to Eq.(8) with estimated parameters of optical saturation power, P_{sat}, and single photon count rate at saturation, ϕ_∞, for the centers at 744 nm (red squares) with P_{sat}=311 μW and ϕ_∞=2.1$\times$10^6 counts/s; at 756 nm (green triangles) with P_{sat}=500 μW and ϕ_∞=3.2$\times$10^5 counts/s; at 764 nm (black circles) with P_{sat}=40 μW and ϕ_∞=1.3$\times$10^6 counts/s. For the center at 749 nm (blue diamonds) the saturation curve was fit by Eq.(9) with the estimated values $r_{21}, r_{12}, r_{31}, r_{23}$ and η. From the fit a quantum efficiency of η_{QE}=0.24 is obtained.

moderately low quantum efficiency.

In general two level emitters possessed a ZPL with a FWHM of $\sim$ 10 nm, whilst the three level emitters exhibited a FWHM of $\sim$ 4 nm. The variation of the lifetime (4 ns to 14 ns) of the two level system emitters can be attributed to nanocrystals geometry experiencing local modification of electric field and/or differences in the atomic structure.

The single emitting centres in the range 740-770 nm are believed to arise from chromium atoms within the diamond lattice. The charge state of the chromium complex and number of atoms involved is unknown. The explanation of what leads to two or three level behavior of a particular crystal is still under investigation. One may assume that the strain within the crystal may have a significant effect. Indeed, it was shown for NV centers that strain can modify the transition from being spin conserving to a Λ system geometry[23]. Similarly, the strain can modify the electronic transition and enhance/suppress the relaxation to a third metastable state.

5. Conclusion

A full optical characterization of the photophysics of novel optical centers attributed to chromium related defects in sub-micron CVD grown diamond crystals was performed. Novel two-level systems with ZPLs at 744 and 764nm, were identified and characterized. The direct measurement of the total collection efficiency from the two level systems enabled a more accurate determination of the quantum efficiency of the three level single emitter at 749 nm (η_{QE}=0.24).

The spectral width of the two level emitters was $\sim$ 10 nm, whilst the three level emitter exhibited a FWHM of $\sim$ 4 nm. This coupled with the short excited state lifetimes (1-14 ns) and

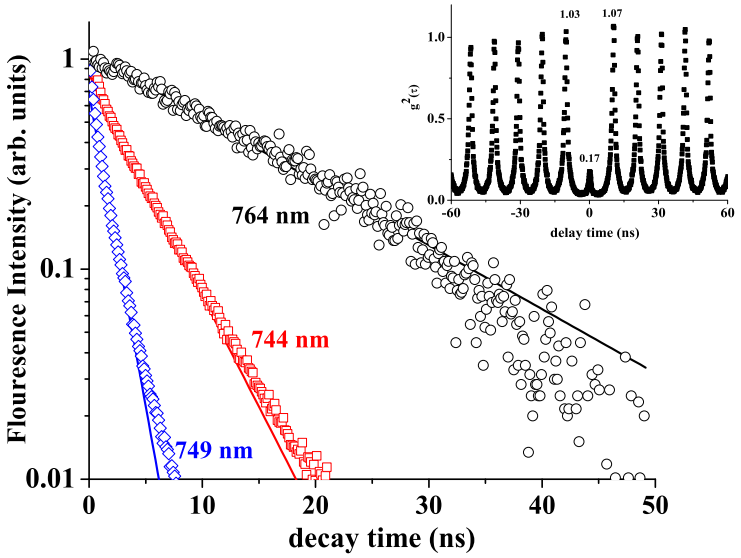

Fig. 7. Direct measurement of the lifetime for the centers at 744 nm (red squares), 749 nm (blue diamonds) and 764 nm (black circles), using a pulsed laser at 20 MHz repetition rate with 200 ps pulse width. The data were fit with a single exponential. The deduced lifetimes of the centers are respectively 4.1 ns, 1.4 ns and 14.2 ns. Inset: Anti-bunching measurement recorded from a single emitter at 749 nm under pulsed laser excitation at 40 MHz and average power of 70 μW.

the high brightness (up to MHz regime), brings these diamond centers much closer to an "ideal single photon source on demand". The precise engineering of two-level single photon emitters may lead to such sources being implemented as a single photon standard.

6. Acknowledgment

This work was supported by the Australian Research Council, The International Science Linkages Program of the Australian Department of Innovation, Industry, Science and Research (Project No. CG110039) and by the European Union Sixth Framework Program under the EQUIND IST-034368. ADG is the recipient of an Australian Research Council Queen Elizabeth II Fellowship (project No. DP0880466).